Supporting information

Mechanistic study on thermally-induced lattice stiffening of ZIF-8

Jian Hao,[a] Deepu J. Babu,[a] Qi Liu,[a] Pascal Alexander Schouwink,[b] Mehrdad Asgari,[c] Wendy L. Queen,[c] and Kumar Varoon Agrawal[a]*

[a] Laboratory of Advanced Separations (LAS), École Polytechnique Fédérale de Lausanne (EPFL), Rue de l'Industrie 17, CH-1951 Sion, Switzerland
[b] Institut des Sciences et Ingénierie Chimiques, EPFL, Rue de l'Industrie 17, CH-1951 Sion, Switzerland
[c] Laboratory for Functional Inorganic Materials (LFIM), EPFL, Rue de l'Industrie 17, CH-1951 Sion, Switzerland

Corresponding author: E-mail: kumar.agrawal@epfl.ch

Note S1: Heating environment

The heating environment for the post-synthetic rapid heat treatment (RHT) on ZIF-8 membranes in this work are classified as follows:

a) Humid air: The humidity level is referred to as the amount of water vapor (WV) in the air exposed to ZIF-8. This is approximated to be the same with that in the ambient environment in our laboratory where the temperature is 23 ℃, and the relative humidity fluctuates between 30-40%, corresponding to a WV fraction of 0.8-1.1%. For the sake of simplicity, we term this as 1.0% H_2O content in air.

b) 6.2% WV: To increase the WV fraction for the dedicated experiments, we bubbled air through a heated water bath (70 ℃) and then introduced the resulting air into the tubular furnace (Figure S6a). Since the tube is at atmospheric pressure under humid air, the composition of the water vapor inside the tube can be calculated by subtracting the air fraction monitored by an O_2 sensor (OXY-Flex-1H, SST Sensing Ltd., Figure S6b). Figure S6c shows the normalized O_2 content measured at the sample position in the tube at 300 ℃. The oxygen content decreases immediately after inserting the sensor into the tube and shortly stabilizes at 19.7%, which means that the water vapor inside the tube is around 6.2%.

c) Argon: Dry, high purity argon was used from a gas cylinder.

Note S2: Thermal shrinkage kinetics

The thermal shrinkage of ZIF-8 treated in air_1.0%H_2O and argon shows a linear correlation versus time. The intercept when the shrinkage is zero corresponds to the induction time of ZIF-8 thermal shrinkage. In our study, the induction time is negligible compared with the 120 min (2 h) of heating. Thus, the ZIF-8 shrinkage kinetics follow the below equation:

$$\frac{d(shrinkage)}{dt} \approx \frac{Shrinkage}{t} = k(T) = Ae^{-E_a/RT} \quad (1)$$

where t is the heating time, E_a is the activation energy of the ZIF-8 thermal shrinkage, and A is the pre-exponential factor.

Note S3: Chemical reactions of ZIF-8 during heat treatment

i. Decomposition: ZIF-8 decomposes after heating in a dry atmosphere (argon/air) normally above 400 °C.[1]

ii. Linker vacancy defects: This is likely to happen, when ZIF-8 is exposed to a mildly humid atmosphere (air_1.0%H_2O) at 300 °C, with linker removed leading to the formation of open metal sites[2].

iii. Hydrolysis of ZIF-8 happens after heating in an extremely humid atmosphere (air_6.2%H_2O) at ~200 °C.[3]

Experimental

Characterizations: Scanning electron microscopy (SEM, FEI Teneo) images were acquired at an accelerating voltage of 1 kV. The diffraction data of ZIF-8 powder before and after the heat treatment was collected in Bragg Brentano geometry using a Bruker D8 discover diffractometer equipped with a LynxEye XE detector (Cu radiation), between 2θ of 5 and 60 and at a rate of 0.8 min^{-1}. The *in situ* XRD of ZIF-8 powders was measured by heating the sample to 300 ℃ in air and 410 ℃ in N_2, respectively, using a homemade high temperature cell. Unit cell parameters were determined using the Le Bail method and fitting the published cubic ZIF-8 structure (*I*4-3*m*) to diffraction data. Fourier transform infrared spectra (FTIR, PerkinElmer Spectrum two TM) of ZIF-8 powders were collected from 400 to 4000 cm^{-1} by 32 scans at a resolution of 2 cm^{-1}. The *in situ* diffuse reflectance infrared Fourier transform spectroscopy (DRIFTS, PerkinElmer with a Diamond ATR cell) on the ZIF-8 powders was conducted at -123 ℃ after activation at 100 ℃ with CO pressures increasing from 0 to 55 Torr. N_2 adsorption isotherm measurements of ZIF-8 powders treated under different conditions were conducted on a BELSORP-max instrument in the range of 0 to 1 bar.

Gas permeation measurements: A homemade Wicke-Kallenbach cell was used to measure the gas permeance of ZIF-8/AAO membranes. The membrane was sealed with epoxy on an annular stainless-steel disk with a 5 mm diameter hole in the center. During measurement, all the gases were delivered into the membrane cell by pre-calibrated mass flow controllers (MKS Instruments). High purity argon (Ar, 99.999%) was used as the sweep gas. The pressure difference between the feed and the sweep side was 0.4 bar. The membranes were heated at 130 ℃ to remove the absorbed gases and moisture under H_2/Ar atmosphere. The compositions of the permeate gas were analyzed by a calibrated mass spectrometer (Hiden Analytical, HPR-20). All the measurements were recorded after reaching a steady state.

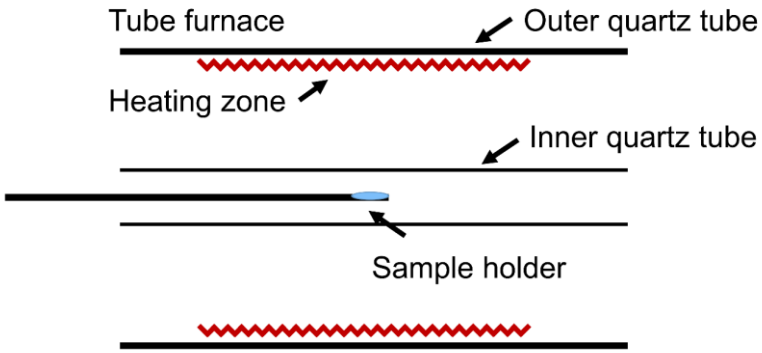

Figure S1. Schematic of the heat treatment setup used in this work.

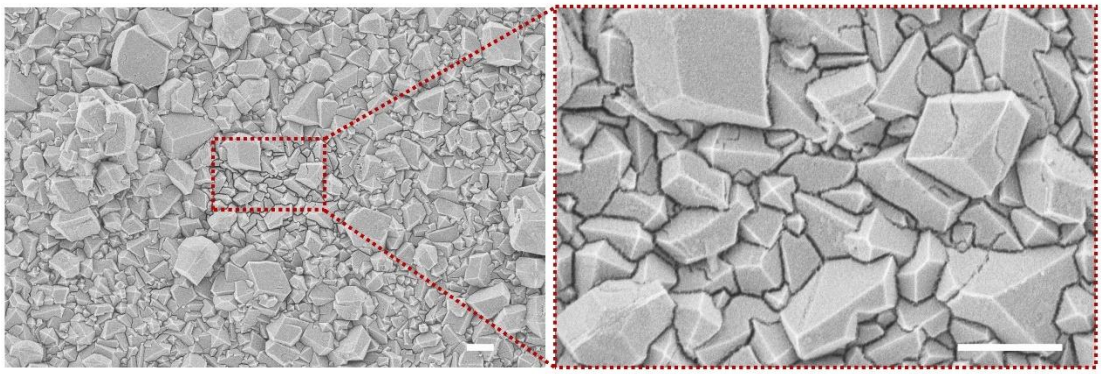

Figure S2. SEM images of the ZIF-8 membrane after heat treatment in air_1.0%H_2O@300C for 18 min. Scale bars correspond to 1 μm.

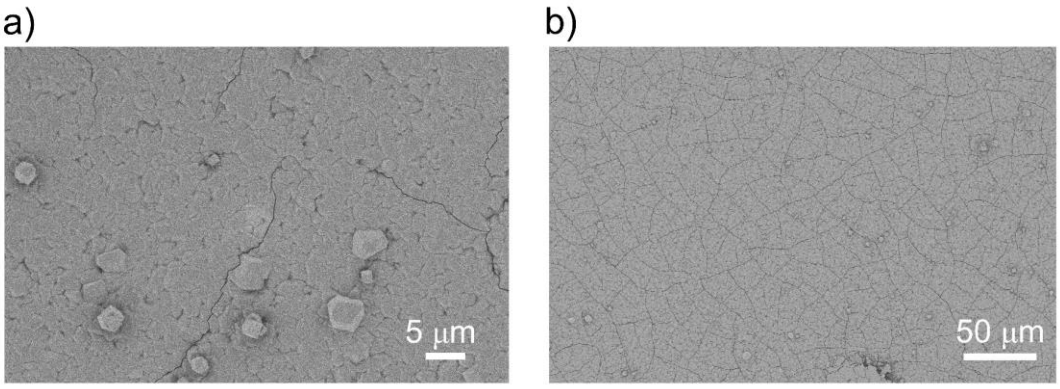

Figure S3. SEM images of the ZIF-8 membrane after heat treatment in air_1.0%H_2O@300C for a) 20 min and b) 30 min. The permeation data of the membrane in panel (b) after PTMSP sealing is as follows: the permeance of H_2 and CO_2 is 5.0×10^{-7} and 4.7×10^{-7} mol m^{-2} s^{-1} Pa^{-1}, respectively, and the H_2/CH_4 and CO_2/CH_4 selectivity is 3.1 and 3.0, respectively.

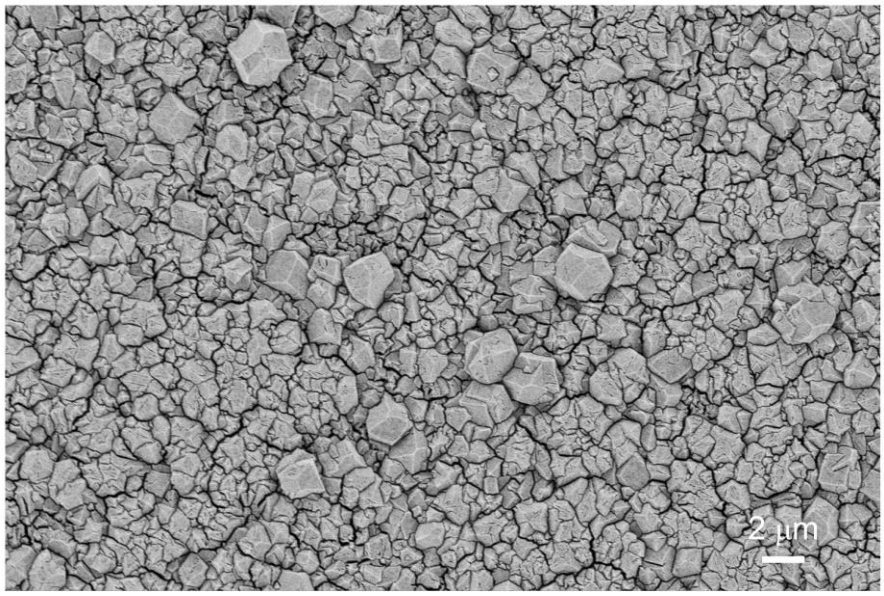

Figure S4. SEM image of the ZIF-8 membrane after heat treatment in air_1.0%H_2O@330C for 10 min.

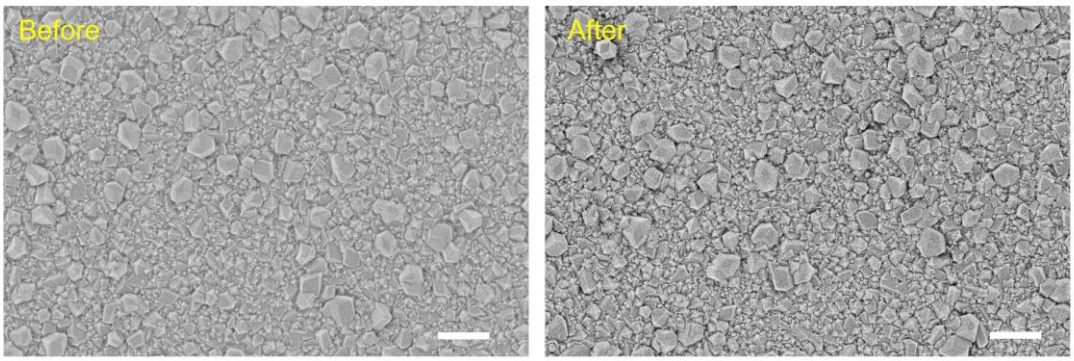

Figure S5. SEM images of the ZIF-8 membrane before and after heat treatment in argon@360C for 10 min. The ramping rate is 50 ℃/min and cooled was carried out by allowing the membrane to cool naturally. Scale bars correspond to 2 μm.

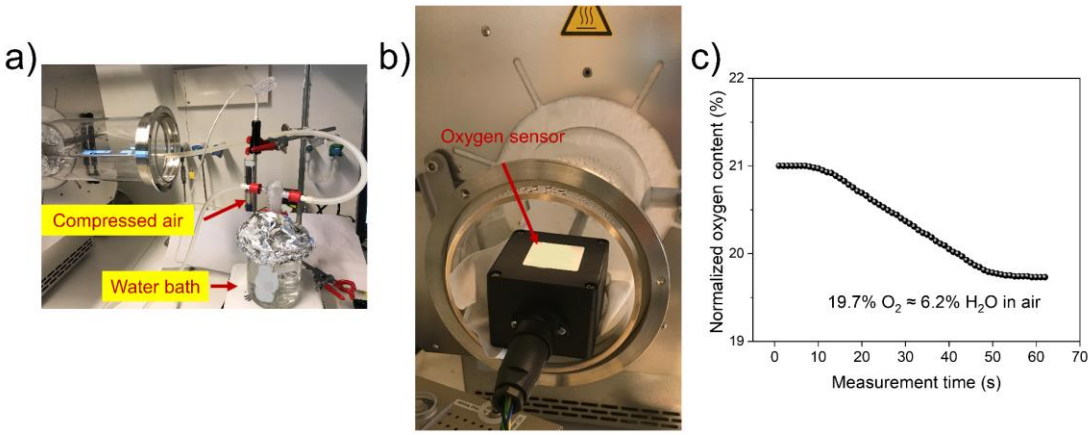

Figure S6. a) The water vapor fraction in the tube is increased by flowing compressed air through a hot water bath (70 ℃) into the (tube) furnace. b) The oxygen sensor used to monitor the oxygen content in the furnace at 300 ℃. c) The calculated water fraction in the tube is around 6.2%.

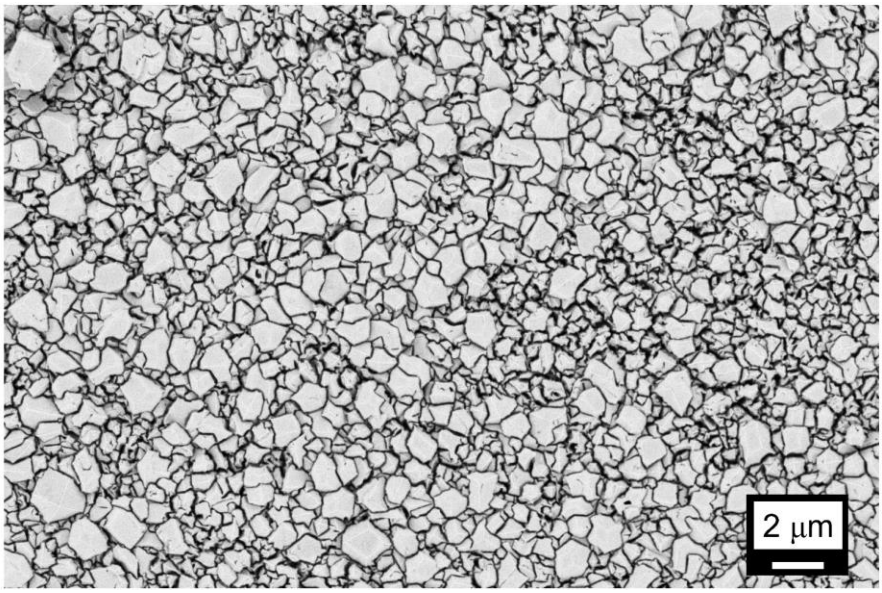

Figure S7. SEM image of the ZIF-8 membrane after heat treatment in air_6.2%H_2O@300C for 10 min.

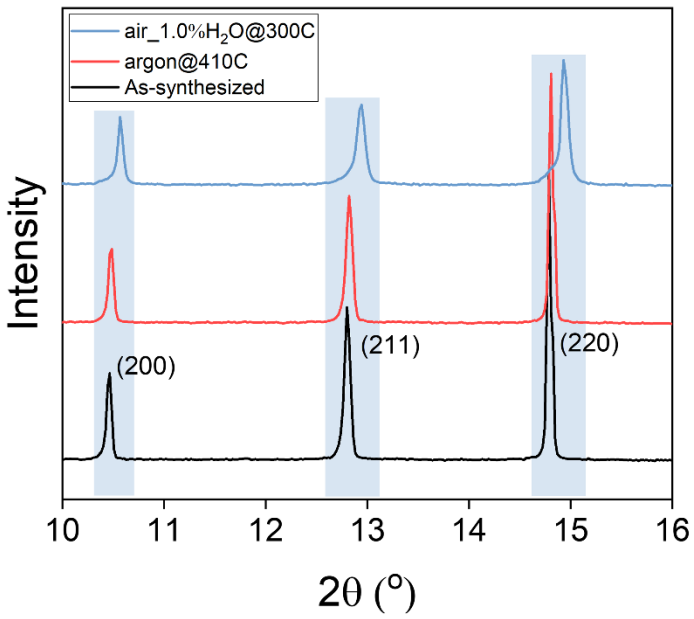

Figure S8. XRD patterns of the as-synthesized ZIF-8 crystals, and those after heating in air_1.0%@300C and argon@410C for 2 h, respectively.

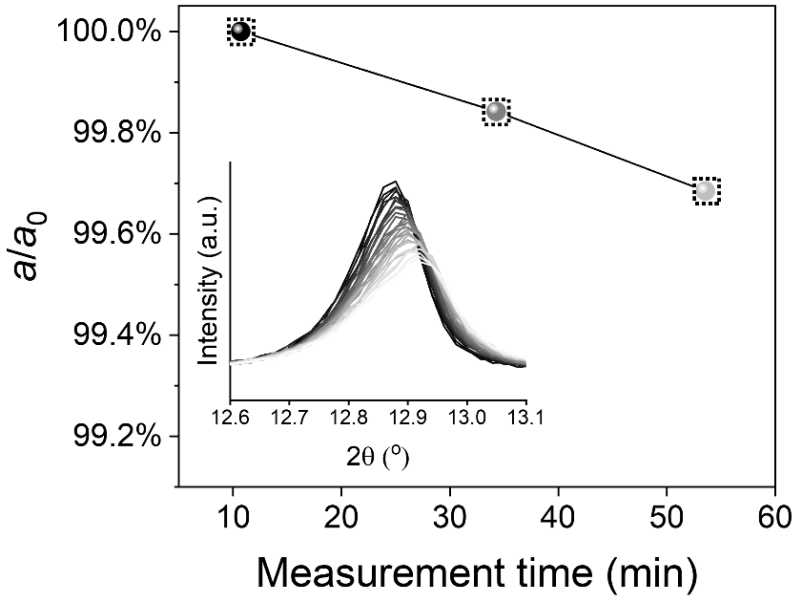

Figure S9. The ratio change of the *a*-axis obtained from *in situ* XRD measurement of ZIF-8 crystals after heating in dry air@300C.

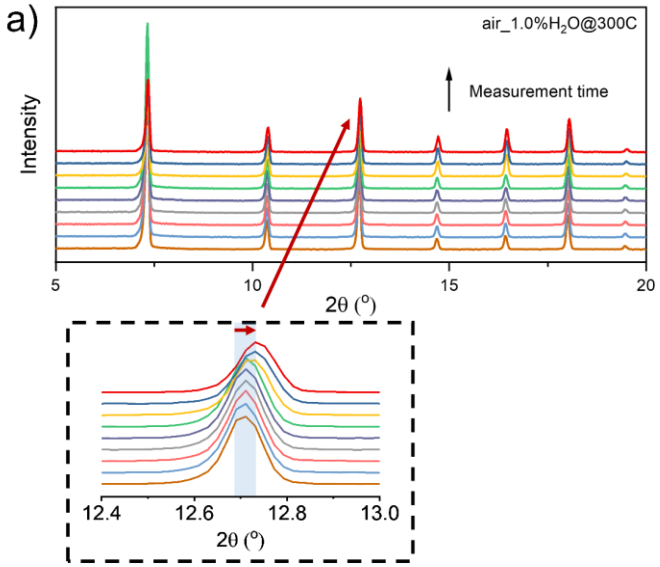

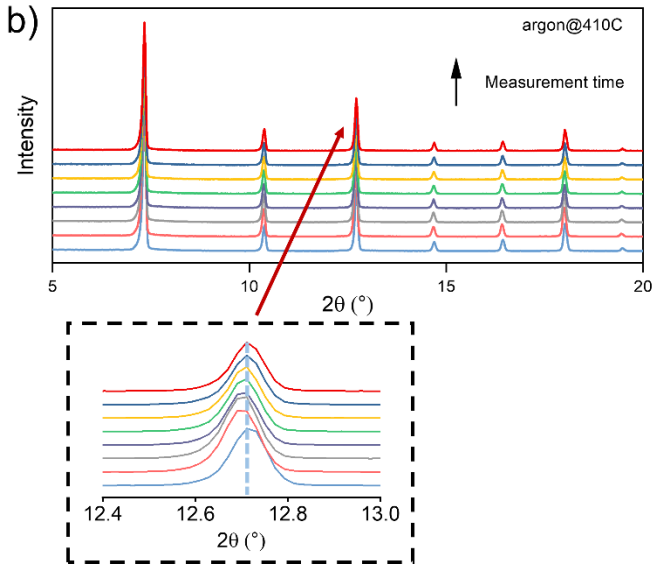

Figure S10. *In situ* XRD patterns of ZIF-8 crystal during heating in a) air_1.0%H_2O@300C, and b) argon@410C, respectively.

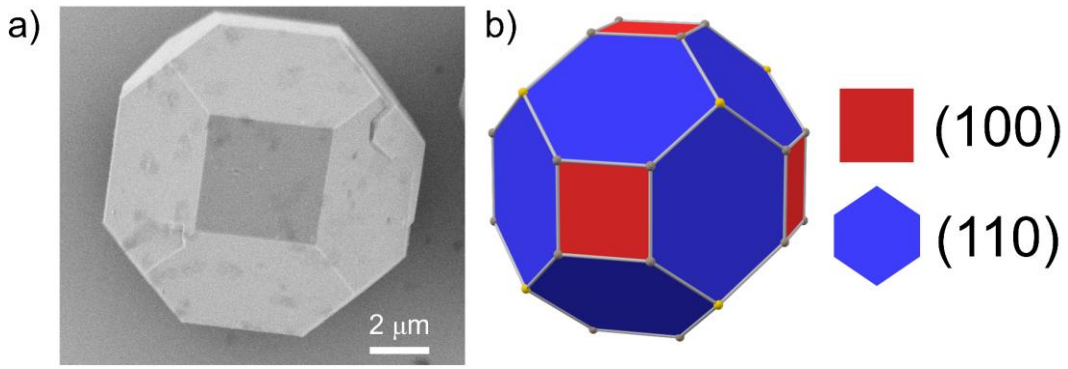

Figure S11. a) SEM image and b) illustration of the crystal morphology of ZIF-8: truncated rhombic dodecahedron with 6 symmetry-equivalent (100) and 12 (110) facets.

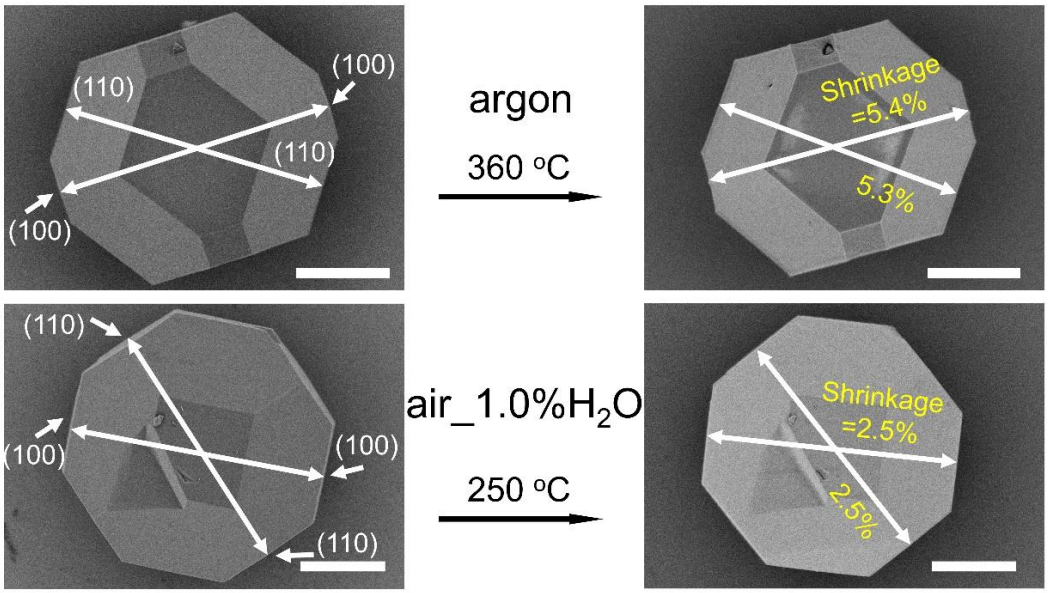

Figure S12. The shrinkage of ZIF-8 after 2 h of heat treatment measured from different facets. Scale bars correspond to 5 μm.

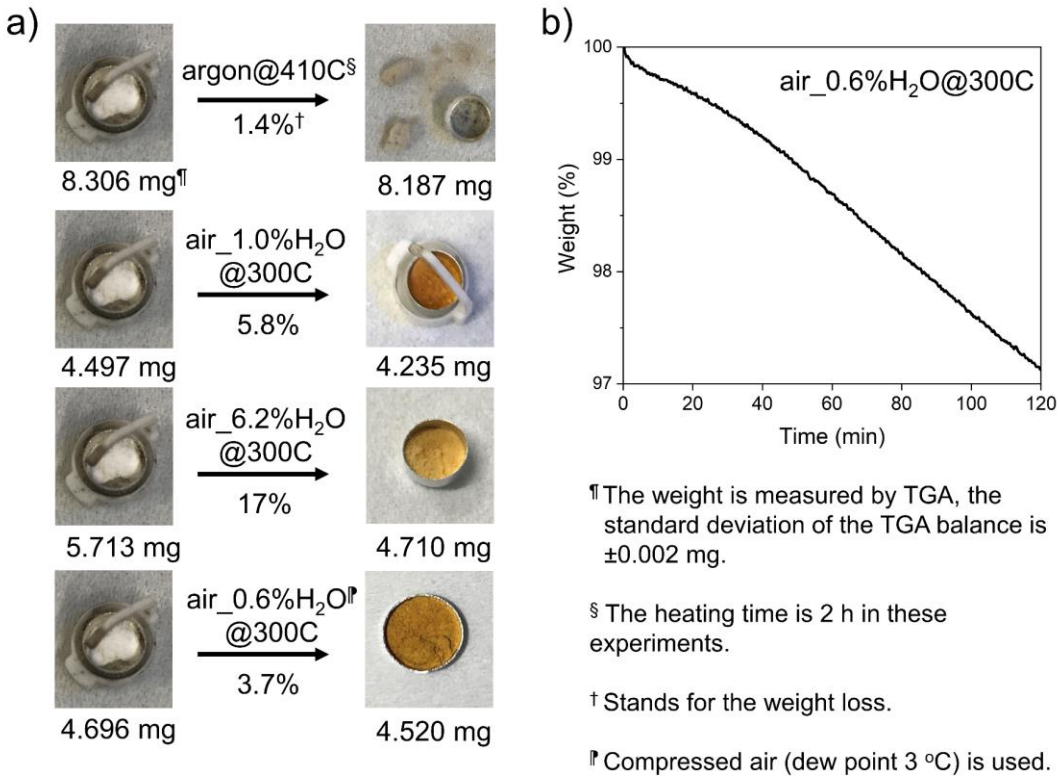

Figure S13. a) Pictures of ZIF-8 powders before and after heating under various conditions for 2h at a heating rate of 5 °C/min, and the corresponding weight loss percentage. b) TGA isothermal curve of ZIF-8 powder heated in compressed air for 2 h. The result is in good agreement with the *ex situ* weight loss measurement.

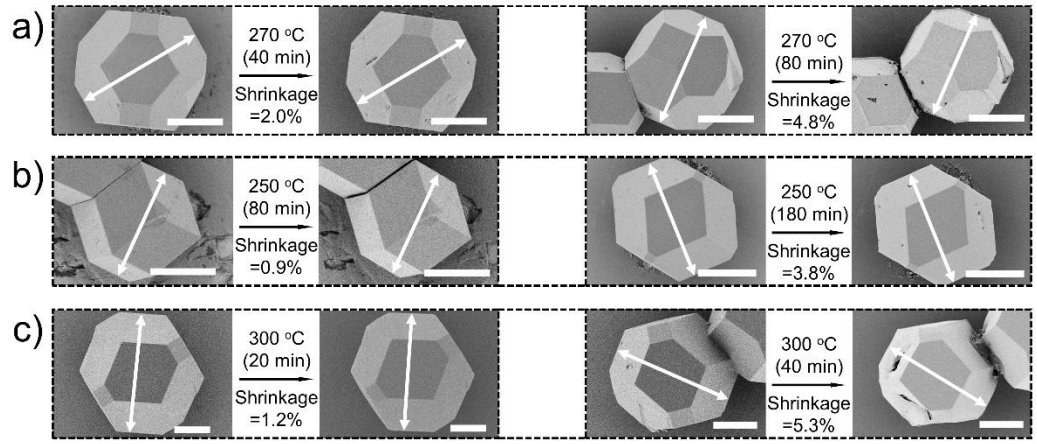

Figure S14. SEM images of ZIF-8 crystals before and after heating in air_1.0%H_2O at a) 270 °C for 40 and 80 min, respectively, b) at 250 °C for 80 and 180 min, respectively, and c) at 300 °C for 20 and 40 min, respectively. Scale bars correspond to 5 μm.

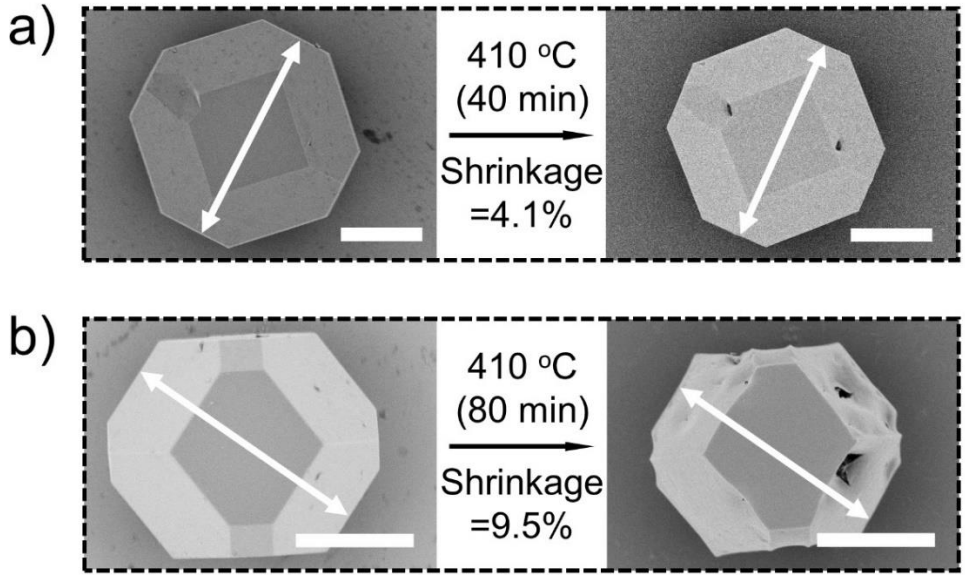

Figure S15. SEM images of ZIF-8 crystals before and after heating in argon@410C for a) 40 and b) 80 min, respectively. Scale bars correspond to 5 μm.

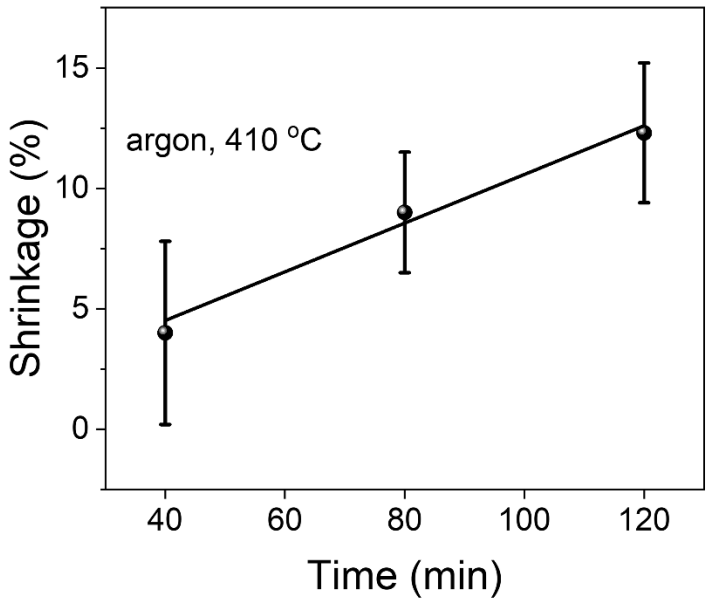

Figure S16. Summarized shrinkage of ZIF-8 crystals treated in argon@410C for 40, 80, and 120 min, respectively.

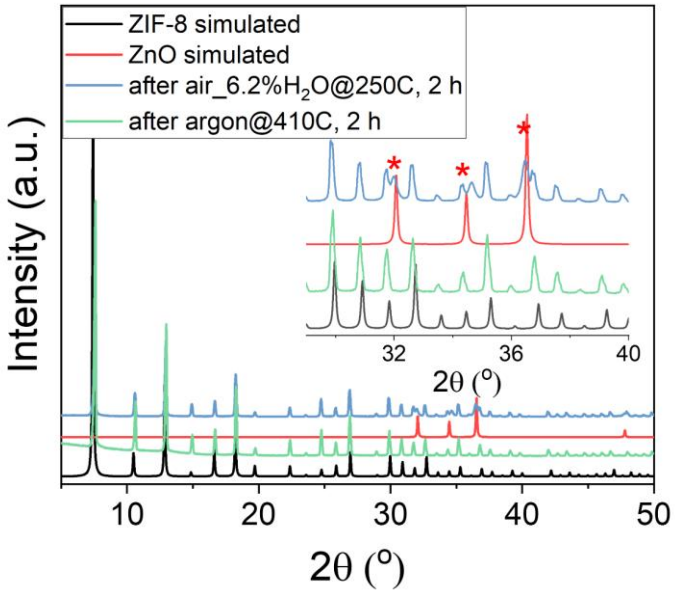

Figure S17. Simulated XRD patterns of ZIF-8 and zinc oxide, and XRD patterns of ZIF-8 after heating in air_6.2%H_2O@250C and argon@410C for 2 h, respectively.

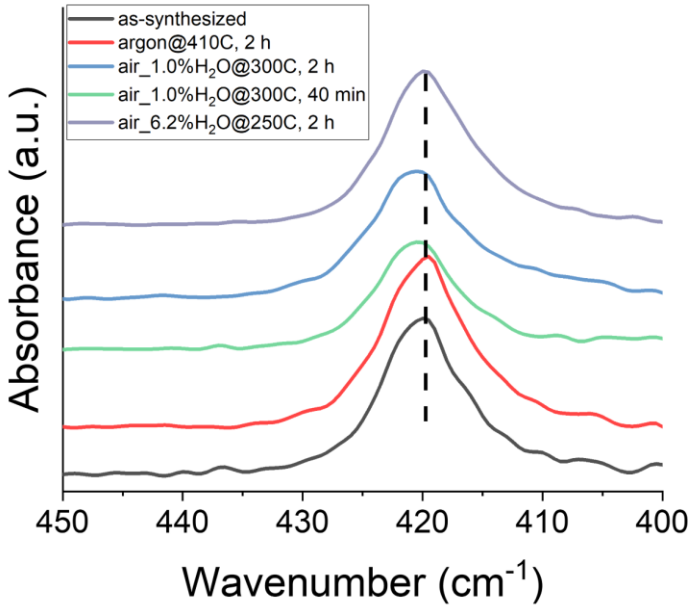

Figure S18. FTIR spectra of ZIF-8 indicating a peak broadening and blue shift of Zn-N bond after heating in air_1.0%H_2O@300C.

Table S1.1. Gas permeance performance of ZIF-8 membranes at 25 ℃ after heating in air_1.0%H_2O@300C.

Sample	Heat treatment duration (min)	H_2 permeance (mol m^{-2} s^{-1} Pa^{-1})		CO_2 permeance (mol m^{-2} s^{-1} Pa^{-1})		Ideal selectivity					
						Before			After		
		Before	After	Before	After	H_2/CH_4	CO_2/CH_4	CO_2/N_2	H_2/CH_4	CO_2/CH_4	CO_2/N_2
M1	3	2.8×10^{-6}	1.8×10^{-6}	5.8×10^{-7}	6.1×10^{-7}	12.8	2.6	3.3	10.8	3.7	4.7
M2	6	2.6×10^{-6}	9.8×10^{-7}	6.2×10^{-7}	4.2×10^{-7}	12.6	3.1	4.1	15.5	6.7	9.6
M3	8	2.6×10^{-6}	9.8×10^{-7}	6.2×10^{-7}	4.2×10^{-7}	12.6	3.1	4.1	25.0	10.4	16.1
M4	10	1.1×10^{-6}	2.3×10^{-7}	3.4×10^{-7}	8.7×10^{-8}	12.4	4.0	4.5	28.7	10.8	14.8
M5	13	1.8×10^{-6}	2.6×10^{-7}	3.9×10^{-7}	9.9×10^{-8}	14.8	3.1	5.2	16.2	6.1	7.6
M6	15	1.8×10^{-6}	6.1×10^{-7}	3.9×10^{-7}	2.9×10^{-7}	14.8	3.1	5.2	9.5	4.6	6.2
M7	18	1.8×10^{-6}	1.2×10^{-6}	3.9×10^{-7}	4.3×10^{-7}	14.8	3.1	5.2	8.2	3.0	4.0
M8	20§	1.4×10^{-6}	2.0×10^{-7}¶	4.0×10^{-7}	-	13.6	4.0	4.3	34.9¶	-	

§ During the 20 min treatment, cracks developed in the membranes. The membrane was covered with a thin layer of Poly(1-trimethylsilyl-1-propyne) (PTMSP) by spin coating a 1.25 wt% PTMSP toluene solution at 1000 rpm for 1 min, and drying at 60 ℃ for 6 h.

¶ Membrane data is collected at 130 ℃. All other data is collected at 25 ℃.

Note:

M2 and M3 were essentially the same membrane which were cut into two pieces for heat treatment experiments. M5, M6, and M7 were essentially the same membrane which were cut into three pieces for heat treatment experiments.

Table S1.2. Gas permeance performance of ZIF-8 membranes at 25 ℃ after heating in air_1.0%H_2O for 10 min.

Sample	Heat treatment condition	H_2 permeance (mol m^{-2} s^{-1} Pa^{-1})	CO_2 permeance (mol m^{-2} s^{-1} Pa^{-1})	Ideal selectivity	
				H_2/CH_4	CO_2/CH_4
M9	260 ℃	1.6×10^{-6}	5.2×10^{-7}	10.2	3.4
M10	270 ℃	2.3×10^{-6}	6.2×10^{-6}	19.0	5.0
M11	280 ℃	1.2×10^{-6}	3.7×10^{-7}	21.2	6.6
M12	300 ℃	7.7×10^{-7}	2.5×10^{-7}	29.5	9.6

Table S1.3. Gas permeance performance of ZIF-8 membranes at 25 ℃ in this work.

Sample	Heat treatment condition	H_2 permeance (mol m^{-2} s^{-1} Pa^{-1})		CO_2 permeance (mol m^{-2} s^{-1} Pa^{-1})		Ideal selectivity					
						Before			After		
		Before	After	Before	After	H_2/CH_4	CO_2/CH_4	CO_2/N_2	H_2/CH_4	CO_2/CH_4	CO_2/N_2
M13	argon@360C for 10 min	4.7×10^{-7}	1.1×10^{-7}	7.0×10^{-8}	1.6×10^{-8}	13.1	1.9	2.3	13.4	2	1.6
M14	air_6.2%H_2O@300C for 3 min	2.4×10^{-6}	6.7×10^{-7}	1.2×10^{-6}	4.8×10^{-7}	13.6	3.8	4.2	14.2	5.9	8.3

Table S2. Peak position in XRD patterns of the as-synthesized ZIF-8, and those after heating in air_1.0%@300C and argon@410C for 2 h, and the ratio changes of *a*-axis lattice parameter calculated by Bragg's law.

		As-synthesized	air_1.0%@300C, 2 h	argon@410C, 2 h
2θ (°)	(110)	7.416	7.498	7.436
	(200)	10.467	10.569	10.487
	(211)	12.801	12.944	12.821
a/a_0 (%)	(110)		98.9	99.7
	(200)		99.0	99.8
	(211)		98.9	99.8

Table S3. Detailed information of the size change of ZIF-8 crystals treated at different conditions. The unit for the size of the crystals is μm.

Number of the crystal		#1	#2	#3	#4	#5	#6	#7	#8	#9	Average
argon@410C for 120 min	Before	10.3	14.5	12.7	13.7	12.7	18.1	12.8	13.4	16.4	
	After	9.2	11.9	10.7	12.1	11.3	16.7	11.4	11.6	14.6	12.3±2.9
	Shrinkage (%)	11.1	17.6	15.7	11.8	10.8	7.9	10.8	13.8	11.2	
argon@410C for 80 min	Before	15.8	15.3	13.3	15.0	14.7	14.4	13.6	11.9	10.8	
	After	14.0	14.1	12.3	13.1	13.2	13.3	13.0	10.7	9.8	9.0±2.5
	Shrinkage (%)	11.3	7.8	7.5	12.2	10.3	7.9	4.5	10.2	9.5	
argon@410C for 40 min	Before	16.0	13.6	9.3	15.0	14.3	16.1	16.5	13.7		
	After	15.5	13.5	8.7	14.3	13.8	15.3	15.6	13.1		4.0±3.7
	Shrinkage (%)	3.0	0.5	6.0	4.6	3.8	4.6	5.3	4.1		
argon@390C for 120 min	Before	12.5	13.7	14.6	16.9	20.8	13.2	15.2	15.1	11.7	
	After	12.0	12.9	13.5	16.1	20.0	12.0	14.0	14.1	10.7	6.3±1.7
	Shrinkage (%)	4.3	5.8	6.9	4.9	3.6	8.8	7.6	6.5	7.9	
argon@360C for 120 min	Before	12.8	12.1	12.6	16.4	16.2	15.9	14.4	12.6	15.0	
	After	12.1	11.5	12.1	16.1	15.6	15.2	13.6	12.0	14.5	4.2±1.0
	Shrinkage (%)	5.7	4.7	3.5	2.0	3.5	4.6	5.8	5.0	3.7	
air_1.0%H_2O @300C for 120 min	Before	10.9	15.7	12.4	12.7	7.4	13.3	13.3	24.7	18.7	
	After	7.7	12.5	9.4	10.0	6.0	10.9	10.3	21.5	15.7	19.8±4.9
	Shrinkage (%)	29.4	20.2	24.5	21.2	18.9	17.8	22.7	13.3	16.0	
air_1.0%H_2O @300C for 40 min	Before	17.3	10.1	15.9	16.5	15.3	16.1	7.6	14.0	13.1	
	After	16.8	9.6	15.5	15.9	14.8	15.1	6.9	13.2	12.5	4.8±2.1
	Shrinkage (%)	3.0	5.0	2.5	3.9	3.5	6.4	9.4	5.3	4.4	
air_1.0%H_2O @300C for 20 min	Before	19.5	12.2	16.7	13.1	13.5	19.3	11.9	15.3	8.7	
	After	19.3	12.0	16.6	13.0	13.3	19.1	11.9	15.1	8.5	1.2±0.6
	Shrinkage (%)	1.1	1.7	1.2	0.7	1.4	1.1	0.5	0.8	2.4	
air_1.0%H_2O @270C for 120 min	Before	9.0	13.7	13.8	10.6	14.4	13.8	13.2	12.6	11.8	
	After	8.6	13.0	13.1	10.0	13.7	13.0	12.5	11.3	10.6	6.4±2.2
	Shrinkage (%)	4.9	5.1	4.8	5.2	5.0	5.7	5.5	10.4	10.6	
air_1.0%H_2O @270C for 80 min	Before	15.9	12.5	11.7	12.6	13.7	17.4	8.8	15.8		
	After	15.1	12.0	11.1	11.8	13.1	16.9	8.4	14.9		4.6±1.0
	Shrinkage (%)	4.8	3.7	5.1	6.4	4.4	3.3	3.8	5.6		
air_1.0%H_2O @270C for 40 min	Before	17.6	17.5	14.8	12.5	11.6	13.6	12.8	8.8	13.3	
	After	17.3	17.1	14.5	12.5	11.4	13.3	12.5	8.6	13.1	2.0±0.6
	Shrinkage (%)	1.4	1.9	2.3	0.7	2.0	2.0	2.4	2.9	1.7	
air_1.0%H_2O @250C for 180 min	Before	10.3	12.9	10.7	13.8	17.1	15.3	13.2	16.8	16.9	
	After	9.9	12.4	10.3	13.5	16.8	14.6	12.7	16.4	16.5	3.0±0.9
	Shrinkage (%)	3.5	3.6	3.5	2.2	1.6	4.4	3.4	2.2	2.4	
air_1.0%H_2O @250C for 120 min	Before	15.8	10.5	16.0	15.4	20.9	18.7	15.7	18.6	22.1	
	After	15.5	10.3	15.8	15.0	20.5	18.4	15.4	18.2	21.9	1.6±0.5
	Shrinkage (%)	1.8	1.6	1.3	2.5	1.5	1.6	1.8	2.0	0.9	
	Before	14.3	13.1	8.8	14.0	11.2	14.7	15.6	15.3		1.0±0.5

air_1.0%H_2O @250C for 80 min	After	14.2	12.9	8.7	13.8	11.0	14.6	15.5	15.2		
	Shrinkage (%)	0.5	1.8	0.9	1.4	1.4	0.4	0.7	1.0		
air@360C for 120 min	Before	16.7	11.6	10.4	18.2	16.5					
	After	15.9	11.0	9.8	17.8	15.9					4.3±1.3
	Shrinkage (%)	4.8	4.9	5.6	2.1	3.9					
air_6.2%H_2O @250C for 120 min	Before	16.5	15.6	17.4	13.0	18.0	14.6	16.1	20.0	12.8	
	After	13.8	14.5	14.6	10.8	15.9	12.6	14.8	18.0	10.8	12.7±3.7
	Shrinkage (%)	16.1	7.3	16.1	16.7	11.6	13.7	7.6	10.1	15.4	
air_6.2%H_2O @220C for 120 min	Before	17.9	16.6	13.3	15.7	16.2	17.4	16.9	15.4		
	After	16.8	15.7	12.5	14.5	15.4	16.5	15.8	14.4		6.1±0.8
	Shrinkage (%)	6.2	5.2	6.3	7.4	5.2	5.1	6.5	6.7		
air_6.2%H_2O @190C for 120 min	Before	16.9	20.4	12.6	12.1	14.0	12.2	13.6			
	After	16.7	20.3	12.3	11.8	13.7	12.0	13.2			1.8±0.8
	Shrinkage (%)	1.5	0.3	2.2	2.3	1.9	1.9	2.9			

Table S4. Kinetic parameters of ZIF-8 thermal shrinkage under different conditions.

Condition	Kinetic parameters		
	$k(T)$ (0.01 min^{-1})	E_a (kJ mol^{-1})	A (0.01 min^{-1})
air_1.0%H_2O@250C	2.0×10^{-2}		
air_1.0%H_2O@270C	5.6×10^{-2}	112±5	3.0×10^{9}
air_1.0%H_2O@300C	1.9×10^{-1}		
Activation energy calculated after approximation in Note S2			
air_1.0%H_2O@250C	1.4×10^{-2}		
air_1.0%H_2O@270C	5.3×10^{-2}	123±18	3.0×10^{10}
air_1.0%H_2O@300C	1.7×10^{-1}		
argon@360C	3.5×10^{-2}		
argon@390C	5.2×10^{-2}	74±22	4.4×10^{4}
argon@410C	1.0×10^{-1}		
air_6.2%H_2O@190C	1.5×10^{-2}		
air_6.2%H_2O@220C	5.1×10^{-2}	65±7	3.6×10^{5}
air_6.2%H_2O@250C	1.1×10^{-1}		

Table S5. BET specific surface area and pore volume of the as-synthesized ZIF-8 and those after heat treatment under different conditions.

Sample condition	BET specific surface area (m^2 g^{-1})	Pore volume (cm^3 g^{-1})
As-synthesized	1450	0.578
air_1.0%H2O@300C, 40 min	1478	0.565
air_1.0%H2O@300C, 2 h	1200	0.542
argon@410C, 2 h	1450	0.545

References:

(1) James, J. B.; Lin, Y. S. Kinetics of ZIF-8 Thermal Decomposition in Inert, Oxidizing, and Reducing Environments. *J. Phys. Chem. C* **2016**, *120* (26), 14015–14026.

(2) Zhang, C.; Han, C.; Sholl, D. S.; Schmidt, J. R. Computational Characterization of Defects in Metal–Organic Frameworks: Spontaneous and Water-Induced Point Defects in ZIF-8. *J. Phys. Chem. Lett.* **2016**, *7* (3), 459–464.

(3) Zhang, H.; Liu, D.; Yao, Y.; Zhang, B.; Lin, Y. S. Stability of ZIF-8 Membranes and Crystalline Powders in Water at Room Temperature. *J. Memb. Sci.* **2015**, *485*, 103–111.